AD-A077 650 PENNSYLVANIA STATE UNIV UNIVERSITY PARK MATERIALS RE--ETC F/G 20/2
TEMPERATURE COMPENSATED PIEZOELECTRIC OXIDE MATERIALS.(U)
SEP 79 G R BARSCH , K E SPEAR F19628-77-C-0131

UNCLASSIFIED RADC -TR-79-219 NL

| OF |
ADA
077650

END
DATE
FILMED
1 -80
DDC

RADC-TR-79-219
Final Technical Report
September 1979

TEMPERATURE COMPENSATED PIEZOELECTRIC OXIDE MATERIALS

The Pennsylvania State University

G. R. Barsch
K. E. Spear

ROME AIR DEVELOPMENT CENTER
Air Force Systems Command
Griffiss Air Force Base, New York 13441

This report has been reviewed by the RADC Information Office (OI) and is releasable to the National Technical Information Service (NTIS). At NTIS it will be releasable to the general public, including foreign nations.

RADC-TR-79-219 has been reviewed and is approved for publication.

APPROVED: Robert M. O'Connell

ROBERT M. O'CONNELL, CAPT, USAF
Project Engineer

APPROVED: Allan C. Schell

ALLAN C. SCHELL
Chief, Electromagnetic Sciences Division

FOR THE COMMANDER: John P. Huss

JOHN P. HUSS
Acting Chief, Plans Office

If your address has changed or if you wish to be removed from the RADC mailing list, or if the addressee is no longer employed by your organization, please notify RADC (EEA), Hanscom AFB MA 01731. This will assist us in maintaining a current mailing list.

Do not return this copy. Retain or destroy.

UNCLASSIFIED

SECURITY CLASSIFICATION OF THIS PAGE (When Data Entered)

REPORT DOCUMENTATION PAGE

READ INSTRUCTIONS BEFORE COMPLETING FORM

1. REPORT NUMBER: RADC-TR-79-219	2. GOVT ACCESSION NO.
3. RECIPIENT'S CATALOG NUMBER	
4. TITLE (and Subtitle): TEMPERATURE COMPENSATED PIEZOELECTRIC OXIDE MATERIALS	5. TYPE OF REPORT & PERIOD COVERED: Final Technical Report 23 Feb 77 — 30 Nov 78
6. PERFORMING ORG. REPORT NUMBER: N/A	
7. AUTHOR(s): G. R. Barsch, K. E. Spear	8. CONTRACT OR GRANT NUMBER(s): F19628-77-C-0131
9. PERFORMING ORGANIZATION NAME AND ADDRESS: The Pennsylvania State University, Materials Research Laboratory, University Park PA 16802	10. PROGRAM ELEMENT, PROJECT, TASK AREA & WORK UNIT NUMBERS: 61102F, 23055520
11. CONTROLLING OFFICE NAME AND ADDRESS: Deputy for Electronic Technology (RADC/EEA), Hanscom AFB MA 01731	12. REPORT DATE: September 1979
	13. NUMBER OF PAGES: 50
14. MONITORING AGENCY NAME & ADDRESS (if different from Controlling Office): Same	15. SECURITY CLASS. (of this report): UNCLASSIFIED
	15a. DECLASSIFICATION/DOWNGRADING SCHEDULE: N/A

16. DISTRIBUTION STATEMENT (of this Report)

Approved for public release; distribution unlimited.

17. DISTRIBUTION STATEMENT (of the abstract entered in Block 20, if different from Report)

Same

18. SUPPLEMENTARY NOTES

RADC Project Engineer: Capt Robert M. O'Connell (EEA)

19. KEY WORDS (Continue on reverse side if necessary and identify by block number)

Crystal Growth	Temperature Compensated Materials
Ultrasonics	Surface Acoustic Wave Devices
Elastic Constants	Berlinite
Thermoelastic Constants	Lead Potassium Niobate
Piezoelectric Constants	Lithium Metasilicate

20. ABSTRACT (Continue on reverse side if necessary and identify by block number)

In order to search for new temperature compensated materials for surface acoustic wave (SAW) devices with low ultrasonic attenuation and high electromechanical coupling, the following ~~experimental and theoretical~~ investigations were carried out: (Cont'd)

DD FORM 1 JAN 73 1473

UNCLASSIFIED

SECURITY CLASSIFICATION OF THIS PAGE (When Data Entered)

220 750

(1) Crystal growth ~~investigations were carried out~~ for lead potassium niobate (PKN), $Pb_2KNb_5O_{15}$ and for lithium metasilicate, Li_2SiO_3 by using the Czochralski method. For PKN crack free single crystal boules up to 15 mm diameter and 30 mm length were obtained in a resistance furnace. The as-grown crystals contained both 90° (elastic) and 180° (electric) domains which could be removed by strain-annealing in an electric field. However, by the poling process micro cracks are induced. For lithium metasilicate single crystal boules up to 15 mm diameter and 20 mm length were obtained in an induction furnace. Smaller boules were crack free, but larger boules contained cracks. Chemical etching experiments revealed the presence of 180° domains. All efforts to pole the crystals during or after growth were unsuccessful.

(2) The complete set of elastic, dielectric and piezoelectric constants and of their temperature coefficients is reported for unpoled PKN. For bulk waves temperature compensated directions with electromechanical coupling factors up to 0.22 are predicted from these data. For poled PKN the piezoelectric strain constant d_{22} has been measured and found to agree approximately with the value of Yamada (1975). This implies that for poled PKN the coupling factors for the temperature compensated directions may be considerably larger.

(3) The piezoelectric strain constants d_{11} and d_{14} of α-berlinite have been measured by the static x-ray method. The piezoelectric stress constants e_{11} and e_{14} calculated from these results are larger than the values previously determined ultrasonically. For the temperature compensated AT cut of berlinite an electromechanical coupling factor of 0.4 for bulk waves has been calculated from the x-ray data of the piezoelectric constants.

(4) The dielectric constant ε_{33}^{T} and the loss tangent of α-berlinite were measured from 10^3 to 10^6 Hz between -175° and + 200°C. Two relaxation peaks are present in the loss tangent. Their possible causes and their effect on the temperature compensated directions and on the associated electromechanical coupling factors are discussed.

(5) In order to assess the reliability of the x-ray method the piezoelectric strain constants d_{11} and d_{14} of α-quartz were measured with this method. The value obtained for d_{11} is in excellent agreement with the results obtained by other experimental methods. The value of d_{14} obtained from the (024) reflection is about 30 percent larger than the values obtained by other methods, but the value of d_{14} obtained from the $(0\bar{1}2)$ reflection has the wrong sign. Possible reasons for this discrepancy are discussed.

ACKNOWLEDGMENTS

The authors would like to thank their colleagues and collaborators for their participation in this work: Dr. M. Brun, and Mr. R. Berger for the crystal growth investigations, Dr. W. F. Regnault for the property measurements on lead potassium niobate, and Dr. Z. P. Chang for the x-ray determination of the piezoelectric constants of quartz and of berlinite, and for the dielectric constant measurements of berlinite. Our thanks are extended to Professor L. E. Cross for his valuable advice, and for his permission to use the facilities of his laboratory for the dielectric constant measurements.

TEMPERATURE COMPENSATED PIEZOELECTRIC OXIDE MATERIALS

TABLE OF CONTENTS

ACKNOWLEDGMENTS

The authors would like to thank their colleagues and collaborators for their participation in this work: Dr. M. Brun, and Mr. R. Berger for the crystal growth investigations, Dr. W. F. Regnault for the property measurements on lead potassium niobate, and Dr. Z. P. Chang for the x-ray determination of the piezoelectric constants of quartz and of berlinite, and for the dielectric constant measurements of berlinite. Our thanks are extended to Professor L. E. Cross for his valuable advice, and for his permission to use the facilities of his laboratory for the dielectric constant measurements.

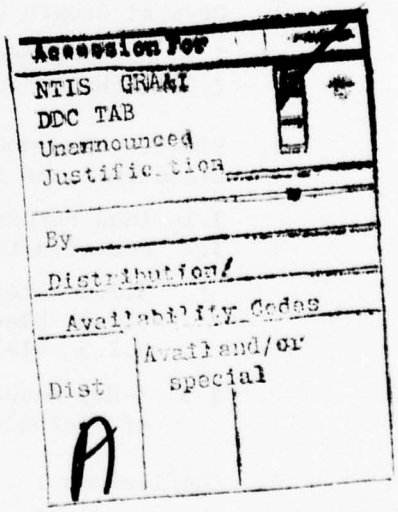

TEMPERATURE COMPENSATED PIEZOELECTRIC OXIDE MATERIALS

TABLE OF CONTENTS

EVALUATION

This is the Final Report on Contract F19628-77-C-0131. It covers research performed during the period of 23 February 1977 to 30 November 1978. The objective of the work was to search for new temperature-compensated materials for surface acoustic wave (SAW) devices with low ultrasonic attenuation and high electromechanical coupling. The work solved some of the crystal growth problems of lead potassium niobate and lithium metasilicate, characterized the thermoelastic behavior of lead potassium niobate, and established the utility of the x-ray method for measuring piezoelectric constants. This work contributes greatly to the very important problem of finding new temperature-compensated SAW materials with piezoelectric coupling as large as that of lithium niobate. The availability of such a material will allow the development of unthermostatted temperature-stable broadband SAW devices.

Robert M. O'Connell

ROBERT M. O'CONNELL, CAPT, USAF
Project Engineer

1. Technical Summary and Progress Report

1.1 Technical Problem and Task Objectives

The objective of the work pursued under this contract is to find new temperature compensated piezoelectric materials for use in ultrasonic SAW signal processing devices, which are superior to α-quartz and α-berlinite, i.e. materials with sufficiently large electromechanical coupling, low ultrasonic attenuation and a vanishingly small temperature coefficient of the delay time.

1.2 Methodological Approach

The research performed consists of

(I) both exploratory and systematic crystal growth studies on materials which were expected to possess temperature compensated crystallographic directions and which had been selected earlier under AFCRL Contract F19628-73C-108 and RADC Contract F19628-75-C-0085 on the basis of certain heuristic criteria (Barsch and Newnham, 1975; Barsch and Spear, 1977).

(II) measurement of the single crystal elastic, thermoelastic, piezoelectric and dielectric properties of promising candidate materials for which suitable single crystals are available and

(III) the theoretical determination of temperature compensated crystallographic directions for ultrasonic bulk waves and their associated electromechanical coupling factors from the experimental data obtained under (II).

Compensated cuts for ultrasonic surface waves for the materials studied and their suitability for SAW devices will be investigated by the scientific staff of the Rome Air Development Center under supervision of the Contract Monitor, Dr. R. M. O'Connell.

1.3 Technical Results

1.3.1 Crystal Growth

Crystal growth was pursued for PKN ($Pb_2KNb_5O_{15}$) and lithium metasilicate (Li_2SiO_3).

1.3.1.1 Lead Potassium Niobate

The crystal growth of PKN was performed largely in a newly built platinum resistance furnace. Its advantages over the previously used equipment were improved temperature control, the capability to modify temperature gradients by suitable heat shields and significantly reduced loss of volatile components. It was possible to grow boules up to 15 mm diameter and 30 mm length with approximately constant diameters. For larger diameters the boules contained

a core which probably consists of heterophase inclusions. All crystals were yellow and transparent. Microprobe analysis showed that the composition of crystals was approximately $Pb_{2.1}K_{0.85}Nb_5O_{15}$. The most serious difficulty encountered was the cracking of the boules during cooling. Since cracks had a definite crystallographic orientation, they were associated with the phase transition. Examination of the boules cooled at different rates under an optical microscope showed that the size of the ferroelectric domains decreased with increased cooling rates. All crystals contain both 90° and 180° domains, which can be removed by strain annealing in an electric field. However, the poled single domain crystals contain microcracks which may be associated with growth-related defects and which are detrimental to the physical property measurements.

1.3.1.2 Lithium Metasilicate

Lithium metasilicate single crystals were grown in an induction heated AD Little furnace. By using seed crystals it was possible to obtain boules up to 15 mm diameter and 20 mm length. The crystals were colorless and transparent. Some difficulties with cracking of the boules were encountered. All crystals exhibited excellent cleavage parallel to the (100) planes, so that it was difficult to obtain large oriented and polished pieces. By means of an etching technique polar domains were found in all crystals with an optical microscope. Attempts were made to pole the crystals during growth by growing them in an electric field, however domains were still detected, because only a low electric field could be maintained. Attempts to pole the crystals by doping the melt with cations which were expected to be rejected by the melt were unsuccessful because these ions were incorporated into the crystal.

1.3.2 Physical Property Measurements and Suitability for Temperature Compensated SAW Devices

1.3.2.1 Lead Potassium Niobate

The work on unpoled PKN initiated under the previous contract from RADC was completed. The complete set of elastic, dielectric and piezoelectric constants, and of their temperature coefficients is reported. For bulk waves temperature compensated directions with electromechanical coupling factors up to 0.22 are predicted from these data on the basis of theoretical calculations. The longitudinal piezoelectric strain constant d_{22} for a poled crystal grown under the present contract has been measured directly with a d_{33}-meter, and a value comparable to that determined by Yamada (1975) for poled PKN has

been found. This implies that for poled PKN the electromechanical coupling factors corresponding to the temperature compensated directions may be considerably larger than for the unpoled material.

1.3.2.2 α-Berlinite

The work on the x-ray determination of the piezoelectric constants initiated under the previous contract from RADC/EEA was continued. From three independent series of measurements of the change of the Bragg angle of the $(2\bar{1}0)$, the $(0\bar{1}4)$ and the (014) reflections consistent values for the two piezoelectric strain constants d_{11} and d_{14} were obtained. The piezoelectric stress constants e_{11} and e_{14} calculated from these values are for right-handed α-berlinite

$$e_{11} = -0.54 \frac{C}{m^2} \pm 4\% \qquad (1a)$$

$$e_{14} = -0.16 \frac{C}{m^2} \pm 18\% \qquad (1b)$$

The value for e_{11} is almost 80 percent larger than the previously determined less accurate ultrasonic value (Chang and Barsch, 1976), and the x-ray value for e_{14} has even the opposite sign than the earlier (very uncertain) ultrasonic value. Whereas for righthanded quartz the signs of e_{11} and e_{14} are opposite ($e_{11} < 0$, $e_{14} > 0$), for righthanded berlinite according to (1a) and (1b) the signs of both constants are negative. As a consequence, the calculated electromechanical coupling factor of α-berlinite for a rotated Y-cut versus the angle of rotation is qualitatively different than for α-quartz in that the minimum occurs for rotations in opposite directions, and in that the value of the coupling factor for the temperature compensated AT cut has the large value of 0.4 and is for berlinite much closer to the maximum value than for quartz. Furthermore, the value of 0.4 is 4.5 times larger than for α-quartz, and 2.6 times larger than for the previously reported value of α-berlinite calculated from the ultrasonic data (Chang and Barsch, 1976). This implies that α-berlinite may be an even better substrate material for SAW devices than concluded previously.

Since the data analysis of the results of the ultrasonic measurements on α-berlinite (Chang and Barsch, 1976) were based on the assumption that the two dielectric constants ε_{11}^T and ε_{33}^T are equal the dielectric constant ε_{33}^T of α-berlinite and the loss tangent have been measured between -175° and +200°C at frequencies of 10^3, 10^4, 10^5 and 10^6 Hz. Two relaxation peaks are present in the loss tangent and are associated with the usual step-like

kinks in the real part of the dielectric constants. The peaks are tentatively attributed to heterophase inclusions with relatively large electrical conductivity. The room temperature value of $\varepsilon_{33}^{T} = 6.32$ at 1MHz is close to the value $\varepsilon_{11}^{T} = 6.05$ reported by Mason (1950). The implications of the relaxation effects in the dielectric constant for the temperature compensated directions and for the associated coupling factors remain to be investigated.

1.3.2.3 X-Ray Method for Determination of Piezoelectric Constants

In order to check the reliability of the x-ray method for measuring the piezoelectric strain constants this method has been applied to α-quartz, for which experimental data obtained by other methods are available. The values obtained are

$$d_{11} = -2.29 \times 10^{-12} \frac{m}{v} \qquad (2a)$$

$$d_{14} = -1.0 \times 10^{-12} \frac{m}{v} \qquad (2b)$$

The value of d_{11} was determined from the $(2\bar{1}0)$ reflection and is in very good agreement with the values obtained by the resonance method, namely (in units of 10^{-12} m/V) 2.29 (Cook and Weissler, 1950) 2.25 (Mason, 1950), and 2.31 (Bechmann, 1958). The value of d_{14} was determined from the (024) reflection and is 10 to 50 percent larger than the values obtained by the resonance method, which range from 0.68 (Cook and Weissler, 1950) to 0.85 (Mason, 1950) (in units of 10^{-12} m/V). It has not yet been possible to obtain consistent values for d_{14} from the $(0\bar{1}2)$ reflection. The reasons for this difficulty are not yet understood. Furthermore, the results of individual runs for d_{11} and especially for d_{14} showed some scatter which could arise from sample inhomogeneity, or from fluctuations of the electric field that are induced by structural imperfections. The reproducibility of the measurements was improved by degassing the specimen in vacuum and performing the measurements in a nitrogen gas atmosphere.

In summary, it can be said that the suitability of the x-ray method has been established for the longitudinal piezoelectric effect which permits the direct measurement of d_{11}. However, for the transverse effect, which is described by a linear combination of d_{11} and d_{14}, both the resonance method and the x-ray method show larger variations, that could arise either from the relative smallness of the effect and/or from the relatively stronger dependence of the transverse effect on structural imperfections or contamination of the specimen.

1.4 DOD Implications

Present and future engineering applications of SAW devices include military (and civilian) communications and Radar systems, such as multichannel communications, secure anti-jam communication for satellites, miniature avionics and electromagnetic counter measures. The main performance limiting factor of current SAW devices is that it has not been possible to simultaneously achieve broad bandwidth which increases with increasing electromechanical coupling factor, and small temperature coefficient of time delay. For applications where temperature compensated performance is essential, as in SAW code correlators and in circulating store devices, quartz has been used as a substrate material, which has a relatively small bandwidth.

For two of the materials investigated under the present contract one may expect the existence of temperature compensated cuts for bulk and surface waves, with substantially larger electromechanical coupling, and bandwidth than for α-quartz. For one of the materials investigated, berlinite, temperature compensated cuts with electromechanical coupling factors for bulk waves 4.5 times larger than for quartz may exist. The second material, lead potassium niobate, could be still better. Thus by replacing quartz as a substrate material in surface acoustic wave (SAW) devices with one of these materials insertion losses can be reduced and the operating frequency and/or bandwidth can be increased. In this manner the efficiency, reliability and capability of military communications and Radar systems utilizing SAW signal processing devices can be significantly improved.

1.5 Implications for Further Research

It has been demonstrated that the search for new temperature compensated materials with properties superior to those of α-quartz through the approach used under the present contract can be successful. One may therefore hope that a continued systematic search for new temperature compensated materials under a future contract could lead to the discovery of even more suitable materials. To this end continued crystal growth efforts are required to obtain suitable (single domain) single crystals for the physical measurements, which are necessary to assess the use of a given material for SAW device applications.

1.6 Special Comments

No special comments are offered at this time.

2. Crystal Growth Results

The crystal growth efforts pursued under the present contract deal with lead potassium niobate (PKN), $Pb_2KNb_5O_{15}$, and lithium metasilicate, Li_2SiO_3. The objective was to explore, develop and apply feasible methods for the growth of high-quality single crystals sufficiently large for the physical property measurements. The approach and the results are described below.

2.1 Lead Potassium Niobate

Following the procedure of Yamada (1973) and Nakano and Yamada (1975) all crystals were grown by the Czochralski technique. Both an induction heated AD Little crystal puller, and a puller equipped with a specially built resistance furnace were used. The induction heated furnace provided good crystal diameter control, however, difficulties were encountered in temperature control and the control of the temperature gradients above the crucible. Also, significant losses of PbO and K_2O due to vaporization were encountered, so that work with this unit was discontinued. Use of the resistance furnace alleviated most of these difficulties.

The design of the resistance furnace is shown schematically in Fig. 1. The main heating element consists of a Pt-20%Rh wire, while the secondary element is kanthal. The purpose of the secondary heating element was to decrease the load on the main element and to improve temperature stability. Temperature could be maintained within $\pm$ 0.2°C and adjusted to within 0.15°C. Temperature gradients above the melt can be varied by means of heat shields in the range from 40 - 80°C/cm.

Two difficulties were encountered originally during the growth of boules: (1) the boule diameter was continuously decreasing with time at constant furnace temperature, and (2) the boule diameter was excessively sensitive to changes in temperature when it was larger than about 5 mm. The first problem is due to the thermal insulating effect of the crystal. Since, as seen in Fig. 1, the crucible is heated from the sides and its bottom is well insulated and in the hottest part of the furnace, the top of the crucible is a major heat sink. When a crystal is present on top of the melt, however, the amount of heat loss is decreased. Hence, the temperature of the melt will rise without effecting the furnace temperature which is sensed by the controlling thermocouple. Therefore, it was found necessary to lower the

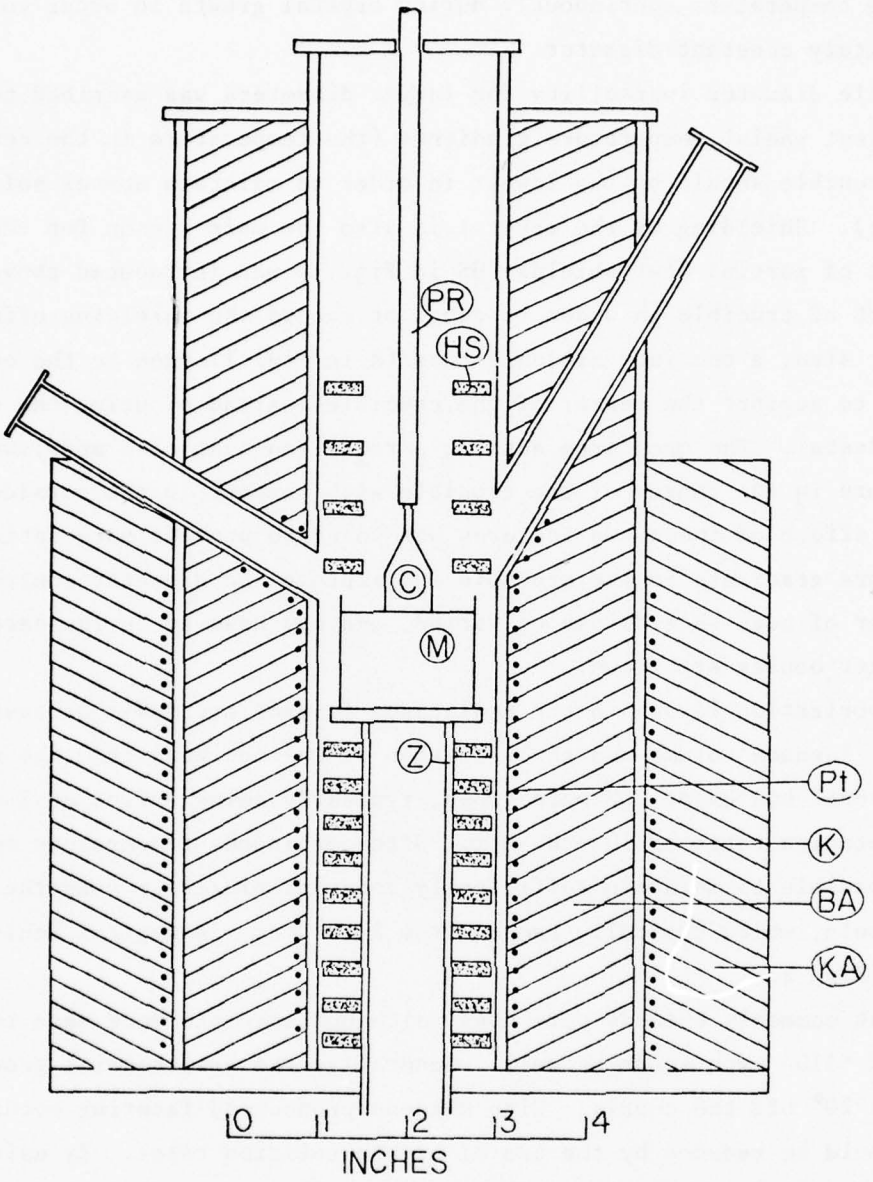

Fig. 1 Cross section of the resistance crystal growth furnace: PR - platinum pulling rod; C - crystal; HS - alumina heat shields; M - melt; Z - zirconia tube; Pt - platinum 20% rhodium furnace winding; K - secondary, kanthal furnace winding; BA - bubbled alumina insulation; KA - kaolin wool insulation.

operating temperature continuously during crystal growth in order to maintain approximately constant diameter.

Boule diameter instability for larger diameters was ascribed to the insufficient radial temperature gradients (the temperature in the center of the crucible should be the lowest in order to maintain convex solid-liquid interface). Shielding by the crystal is also the main reason for this problem, and a set of partial heat shields (HS in Fig. 1) was introduced above the outer part of crucible in order to equal or exceed the shielding effect of the crystal. Also, a one inch zirconia tube (Z in Fig. 1) open to the environment was used to support the center of the crucible instead of using the standard solid pedestal. The open area acts as a radiation heat sink and lowers the temperature in the center of the crucible with respect to the outside. The combined effect of these two features was found to provide more satisfactory temperature gradients in the crucible and improve the diameter control. The number of heat shields can be varied, and may have to be increased when even larger boules are grown.

Vaporization losses in the resistance furnace are small because of the small furnace volume and the isolation of the not zone from the environment.

Several boules of PKN were grown, typically being pulled at 2 - 4 mm/hr and at rotation rates of 10 - 80 rpm. With continuous temperature monitoring it was possible to maintain sufficiently constant diameters over the length of the boule, which typically ranged from 2 to 3 cm. A typical boule is shown in Fig. 2.

Most commonly c-seeds were used, although attempts were made to use <100> and <110> type seeds as well. Generally, the preferential growth direction was about 20° off the c-axis. With c-seeds pronounced faceting occurred, but it could be reduced by the use of higher rotation rates. By using melts with up to 20 wt% PbO and K_2O in excess of the stoichiometric composition, it was possible to grow boules up to 15 mm diameter and 15 mm long. These boules were analyzed by an electron beam microprobe using ceramic standards, and yielded a typical composition of $Pb_{2.1}K_{0.85}Nb_5O_{15}$. Only minor composition changes could be detected along the vertical axis of the boule; horizontal gradients were not detected. Boules grown from melts with excesses of PbO and K_2O were yellow and transparent, boules grown from melts closer to the stoichiometric composition were lighter in color. For boules grown in the induction furnace where volatization was a serious problem, the Pb and K

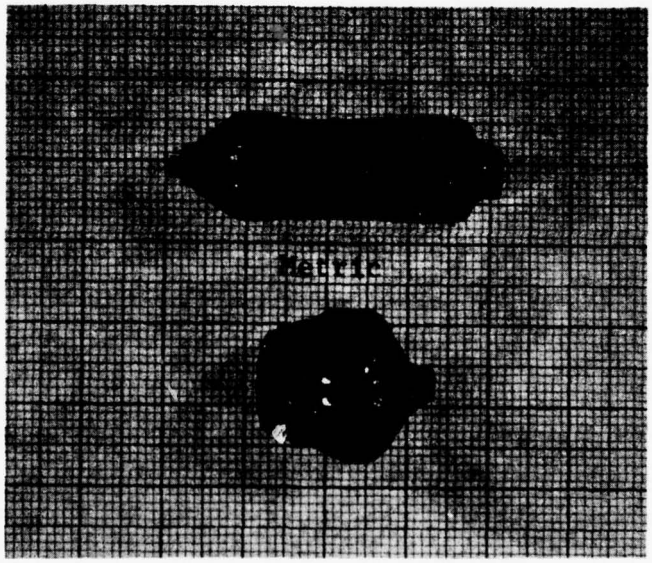

Fig. 2. Typical single crystal boule of PKN

contents were much lower, typically $Pb_{1.98}K_{0.75}Nb_{5.06}O_{15}$. That would indicate that the (Pb + K)/Nb ratio can be decreased below the ideal 3/5, while it could not be higher, as evidenced by the composition of boules grown from melts with excesses of PbO and K_2O.

Extensive cracking of the boules occurred during cooling Most of the cracks were parallel to the crystallographic (001) and (100) planes. This suggests that the phase transformation, rather than thermal shock is responsible for cracking. When polished c-plates of the boules were examined under a polarizing microscope, extensive domain structure was observed. Typical microstructures of boules cooled at different rates through the transformation are shown in Fig. 3-5. It is readily apparent that the size of the domains increases with decreasing cooling rate. The cracking of these boules was also more extensive than in others, which means that the reduction of strain by domain formation is not sufficient to prevent cracking when large domains are formed. It is apparent from Fig. 3 that after heating above the transition and then rapid cooling, some of the domains have increased in extent, while a series of smaller, secondary domains has appeared within the original ones. However, in a rapidly cooled boule, as shown in Fig. 5, the domain structure remained unchanged by cycling through the phase transformation. In all cases, heating crystals 50 - 100°C above the transition was not sufficient to erase the memory effects so that after cooling the domains reappeared in the same positions as before.

The above results indicate that crystals should be cooled at a rather rapid rate ($>$ 200°C/hr) through the phase transition in order to prevent cracking. In the larger boules, however, such cooling rates cause thermal stresses sufficiently large to shatter them.

All crystals grown under the present contract contain the domains apparent from the photomicrographs shown in Figs. 3 to 5. They are 90° (elastic) domains in which the a and b-axes of the orthorhombic low temperature ferroelectric phase of PKN are exchanged (Nakono and Yamada, 1975) In addition, 180° (electric) domains corresponding to the two orientations of the spontaneous polarization along the b-axis must be present roughly in equal amounts but their presence cannot be detected by optical means. Both types of domains were also present in the as-grown crystals of Yamada (1973) and Nakano and Yamada (1975). However, in our earlier crystal growth investigations on PKN (under RADC Contract F19628-75-C-0085) we had obtained single crystal

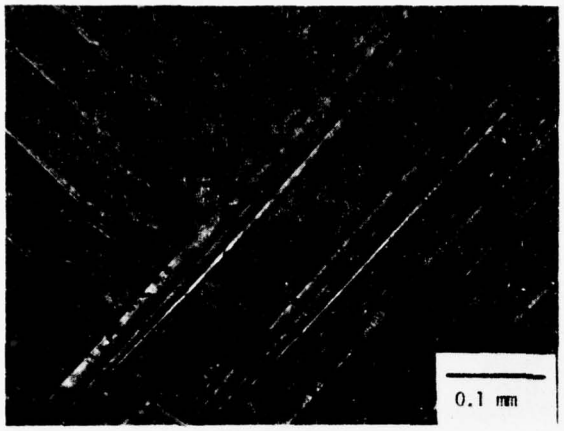

a

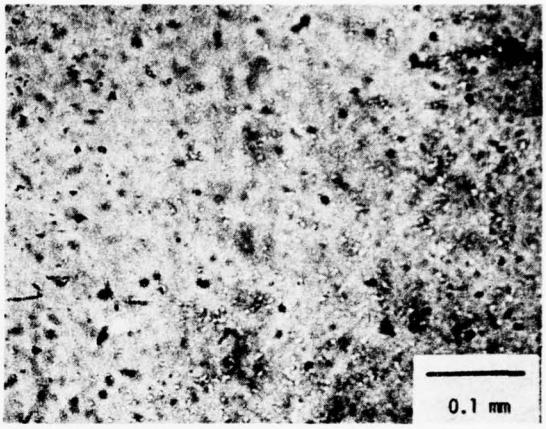

b

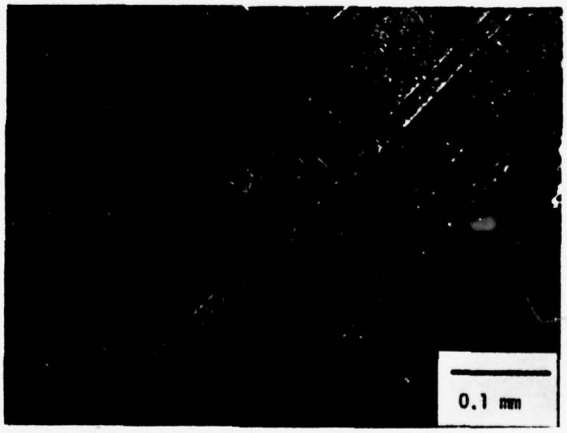

c

Fig. 3 Domain structure of a boule of PKN cooled at the rate of 20°C/hr through the phase transformation, as seen between crossed polarizers.
a - room temperature;
b - 585°C;
c - rapidly cooled from 585°C to room temperature.

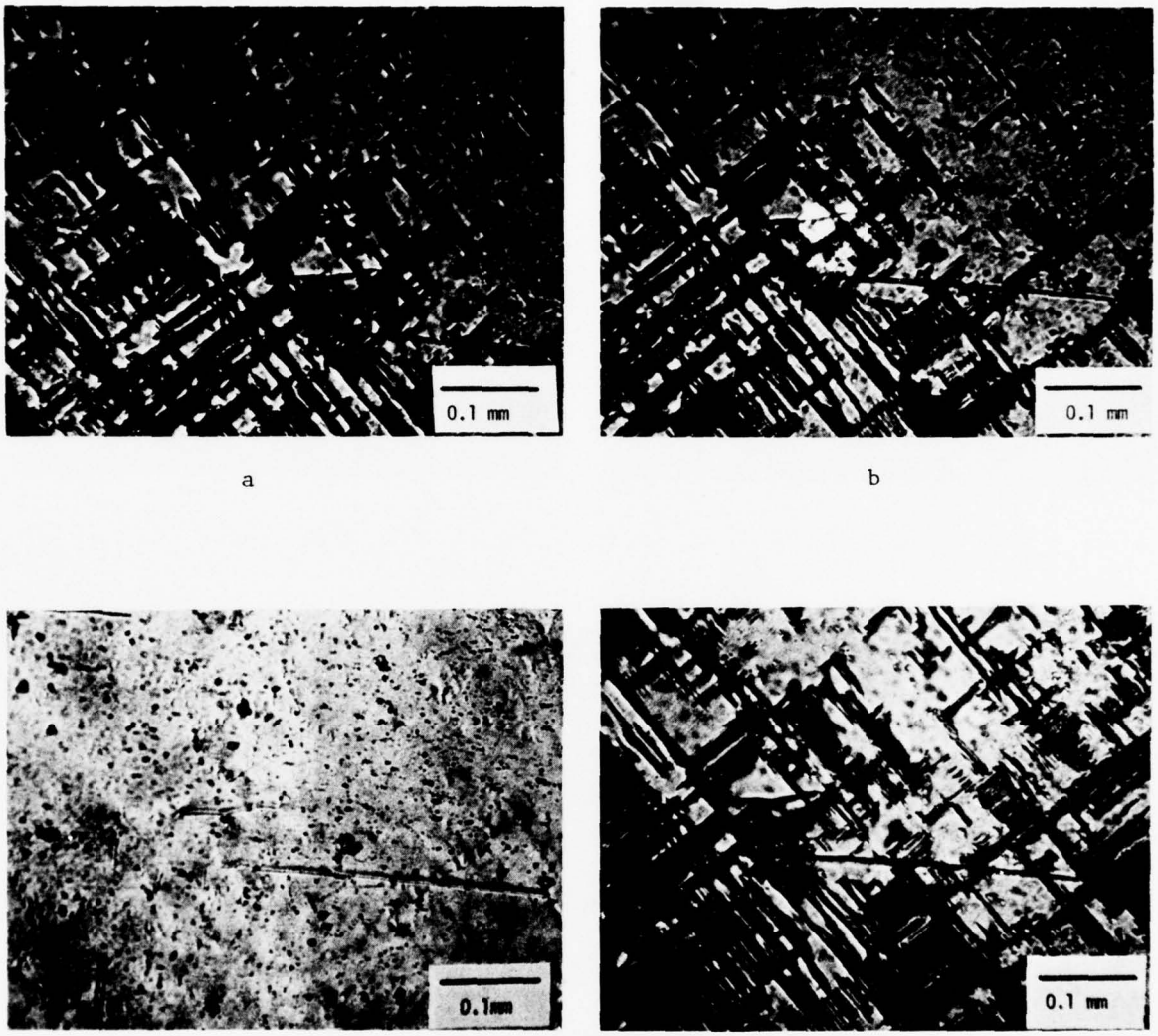

a b

c d

Fig. 4 Domain structure of a boule of PKN cooled at the rate of 50°C/hr through the phase transformation, as seen between crossed polarizers.
a - room temperature;
b - 450°C;
c - 585°C;
d - rapidly cooled from 585°C to room temperature.

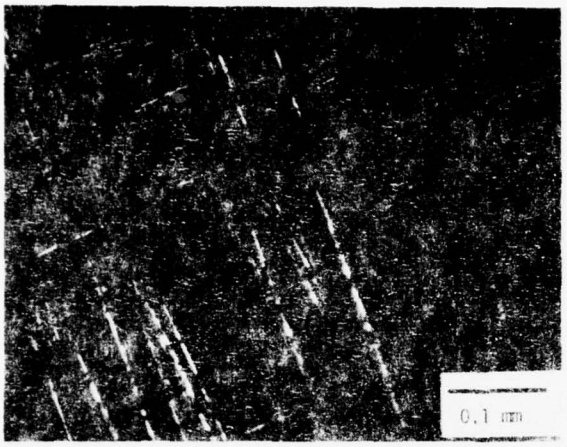

a

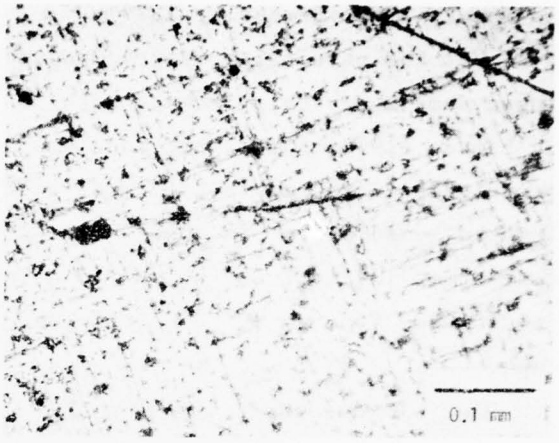

b

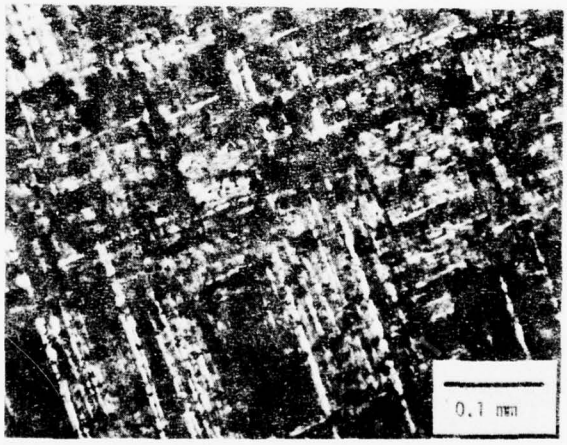

c

Fig. 5 Domain structure of a boule of PKN cooled at the rate of 250°C/hr through the phase transformation, as seen between crossed polarizers.
a - room temperature;
b - 460°C;
c - rapidly cooled from 585°C to room temperature.

boules free of 90° domains which contained small crack-free regions sufficiently large to prepare specimens for the physical property measurements (Barsch and Spear, 1977; Regnault, 1977).

For the physical property measurements and for device applications single domain crystals free of both 90° and 180° domains are required. Following Yamada (1973) and Nakano and Yamada (1975) several rectangular parallelepiped shaped specimen plated with gold electrodes were strain annealed at elevated temperatures in a static electric field. After poling for 20 hours at a stress level of 200 kg/cm^2 at a temperature of 450°C and in an electric field of 200 V/cm no 90° domains could be detected under the polarizing microscope.

The piezoelectric constant d_{22} (referred to a coordinate system with the x_2-axis along the crystallographic b direction) was measured with a Channel Products model CPDT Berlincourt Piezo d_{33}-meter for the samples poled in this manner. The obtained value of 8×10^{-11} m/V is larger than the value of 6.2×10^{-11} m/V reported by Yamada (1975). The closeness of these two values suggests that by the poling in both sets of crystals 180° domains are eliminated to a large extent.

Unfortunately, the strain annealed and poled samples contained microcracks parallel to the 90° domain walls observed earlier which make them unsuitable for the precision measurement of the physical properties.

2.2 Lithium Metasilicate

Growth of lithium metasilicate was performed in the AD Little crystal pulling furnace. Parameters varied were pulling rate, crystal rotation speed, heat shield effects, and seed crystal orientation. Runs were also conducted in which attempts were made to alter the electric potential of the growing system. All boules grown ranged from 15 to 25 mm in length and 10 to 15 mm in diameter.

Preliminary experiments involved nucleation on the Pt wire. A single crystal boule was not obtained, but pieces large enough for use as seeds could be cut from the polycrystalline boules. Subsequently, all experiments were done using seeds oriented either in their original growth direction or in direction 90° away from it.

Pulling rates and crystal rotation were the important parameters in the growth of the boules. It was observed that increasing the pulling rates in order to extract the boules from the melt resulted in the growth of cream-colored translucent material in the lower regions of the boule. These regions

disappeared when the pulling rate was kept constant and extraction was accomplished solely by increasing the temperature. The most transparent boules were grown at pulling rates of 1.5 mm/hr.

Crystal rotation speed was also varied, but after observing the very high viscosity of the melt and the appearance of growth bands perpendicular to the growth direction, runs were made at 30 rpm, the maximum rotation rate of the unit. Some melts were also stirred with a platinum rod before pulling began, but growth bands still occurred. Growth bands were not eliminated by increased seed rotation, but the frequency of their occurrence was reduced significantly.

Cracking of the boules was one of the major problems. It commonly occurred immediately following the extraction of the boules from the melt, but occasionally it occurred at the top of the longer boules even during the growth experiments. Addition of heat shields decreased the cracking but did not eliminate it completely. It is possible that cracking was caused by a phase transition near the melting point. Several DTA experiments were conducted in order to search for such a transition, but results to date were inconclusive. It was attempted to grow crystals from melts at temperatures lower than the melting point of the metasilicate. First, a melt with excess lithium oxide was tried, with a composition intermediate to the stoichiometric metasilicate and the eutectic between the meta- and ortho silicate. The resulting boule, however, contained also some second phase, probably due to the high viscosity of the melt, which did not allow excess lithium oxide to diffuse away from the interface rapidly enough. Lead borate was also tried as a flux. It reduced the melting point and the viscosity of the melt, however, single crystals were not obtained, because some of the flux was again included in the boules.

All boules exhibited cleavage parallel to the (100) planes. The cleavage made it very difficult to obtain large polished and oriented pieces of the crystals because they tended to fall apart in the form of needles and platelets, with [100] in the long direction. Because of the pronounced cleavage, it was originally suspected that fibrous growth occurred. Several runs with [100] type seeds were made, but the boules obtained had the same cleavage properties, indicating that fibrous growth did not take place.

Chemical etching experiments showed the presence of 180° domains in all the crystal boules, and special experiments were designed in an attempt to eliminate these domains during growth through poling. Two kinds of poling

methods were tried. The first consisted of doping the melt with cations which were expected to be strongly rejected by the silicate melt. It was expected that rejected ions would pile up in front of the crystal-liquid interface and cause a high local electrostatic field which should cause all domains to be oriented in the c direction during the growth process. Two cations were tried: Cr^{+} because of its preference for octahedral coordination, and U^{+6} because of its large size and hexavalent charge. It was expected that Cr^{+} would not substitute for Si^{+4}, while its substitution for Li^{+} would require formation of two vacancies. However, when grown in air, apparently Cr^{3+} was oxidized to Cr^{6+}, as evidenced by the deep red color of the melt, and was thus substituted for silicon. The resulting crystal was red in color, and antipolar domains were still observed. Crystals pulled from a melt doped with U^{+6} showed a greenish color, indicating that U^{+6} was not substituted either. Distinctive growth bands parallel to the liquid-solid interface occurred which were either green or colorless transparent in alternating sequence. It is believed that these features resulted from the insufficient homogeneity of the melt, and oversaturation of the melt with U^{+6} ions near the interface. The second poling method attempted consisted of application of a high DC field across the growth interface. For that purpose the seed was painted with platinum paint and held in a platinum pulling rod, grounded to the furnace chamber. The crucible and the melt were connected to the source of DC voltage. Because of the high conductivity of the melt and the crystal, a field of only 200-300 V was required to pass a 10 mA current through the interface. The resulting crystal, however, was not oriented. It is believed that the main reason for this was the inability to maintain sufficiently high fields across the whole assembly.

As-grown crystal boules were colorless and optically transparent, except those doped with chromium or uranium. Small areas in the crystals were sometimes of a milky color. X-ray powder diffraction studies of the small pieces of the crystal boule gave a single phase Li_2SiO_3 diffraction lines, and Laue photographs showed the single crystal nature of the compound. Optical observations indicated high quality of the crystals without any visible inclusions or presence of the second phase in the crystal (see Fig. 6). Conoscopic figures under cross polarized light showed the material was single crystal and of biaxial nature.

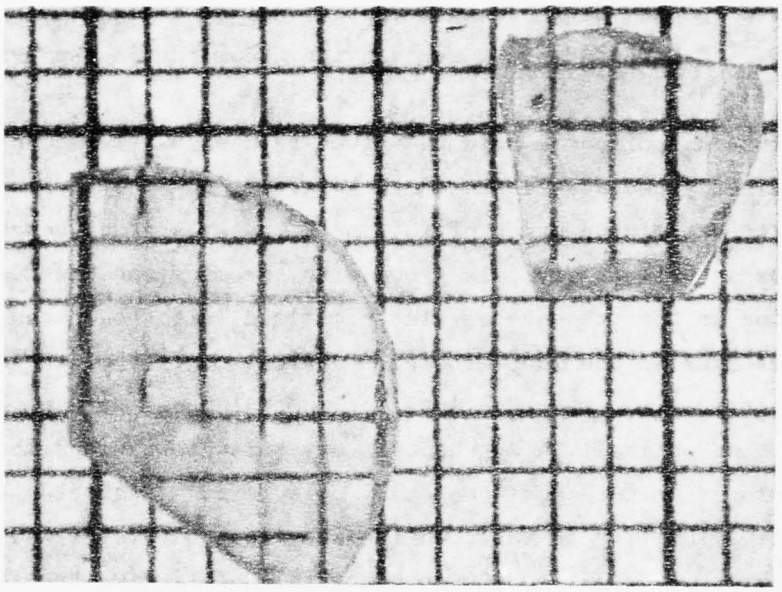

Fig. 6. Two high-quality single crystals of Li_2SiO_3. The small divisions correspond to 1 mm.

Chemical etching experiments were done to study the domain features on c-surfaces of the crystal. Thin plates were cut and polished normal to the pyroelectric c axis of the crystal. Optical examination of these plates under crossed polarized light did not show the presence of domains. When these crystals were lightly etched with dilute acids, e.g. HCl, HF or HNO_3, the 180° domain features were revealed on the surface. The polar nature of the domains was concluded on the basis of d_{33} measurements on the isostructural lithium metagermanate single crystal plates of c-orientation. On a multidomain sample of Li_2SiO_3 the typical values of d_{33} range from 5-10 x 10^{-12} C/N depending on the density of domains in the area of measurements.

Dilute hydrofluoric acid (2 volume percent HF) revealed the domains very distinctly and also attacked the dislocation sites. Dislocation etch pit density was of the order of $10^5/cm^2$. Crystals grown under various growth conditions as well as crystals grown with chromium and uranium impurities and the one in the presence of electric field, all showed the characteristic domain features on chemical etching. Optical quality of the crystals grown under electric field was much superior in that those were highly transparent, colorless and optically homogeneous. Crystals grown with impurities were either colored or were not completely colorless. The boules exhibited no noticeable solubility in water unlike its isostructure Li_2GeO_3 which has solubility in water $\sim$ 1 gm/100 cc. Crystals of Li_2SiO_3 are relatively softer with a hardness between 3 and 4 on Moh's hardness scale.

3. Elastic, Thermoelastic, Piezoelectric, Dielectric and Electromechanical Properties

3.1 Lead Potassium Niobate

Lead potassium niobate, $Pb_2KNb_5O_{15}$, occurs in the tungsten bronze structure and belongs to the orthorhombic crystal class mm2 (C_{2v}). It is ferroelectric, with the spontaneous polarization along the b-axis and a Curie temperature of 450 ± 10°c (Nakano and Yamada, 1975). Electromechanical coupling factors as large as 0.73 have been reported (Yamada, 1973; 1975). Since the temperature coefficients of the resonant frequencies of different crystal cuts have opposite signs (Yamada, 1975) one may expect this material to be temperature compensated for intermediate directions.

Under the previous contract F19628-75-C-0085 the three linear thermal expansion coefficients, the nine elastic constants $c^E_{\mu\nu}$, the five piezoelectric stress constants $e_{i\mu}$ and the three dielectric constants ε_{ij} have been measured as a function of temperature between room temperature and 100°C. The results at 20°C have been reported before (Barsch and Spear, 1977). Under the present contract the data analysis has been extended to include the temperature dependence. The results for the elastic, piezoelectric and dielectric constants, and for their temperature coefficients are shown in Table 1. The orientation of the coordinate system is the same as described before (Barsch and Spear, 1977). For completeness the room temperature values of Yamada (1975) and the three lattice parameters and the associated linear thermal expansion coefficients are also included. The data in Table 1 were obtained on crystals grown in this laboratory which did not contain 90° (elastic) domains, but which apparently contained 180° (electric) domains. This is apparent from the fact that the piezoelectric constant d_{22} of a b-cut specimen as measured with a d_{33} meter is zero, and from the fact that the free dielectric constant ε_{22} is about 10 times larger than the value of Yamada (1975). Attempts to pole the crystals were unsuccessful, apparently because of the absence of 90° domains, although originally this was considered to be an advantage since it assured that the crystals were free of any detectable internal stresses. Since the only effect of 180° domains on the piezoelectric stress constants $e_{i\mu}$ is a sign reversal of some of these constants, and since the $e_{i\mu}$ enter the piezoelectric stiffening term in the Kristoffel tensor quadratically the presence of 180° domains should not affect the ultrasonic velocities if the domain dimensions are large compared with the wavelength of the ultrasonic waves. According to Table 1 piezoelectric constants measured ultrasonically on the unpoled crystals are roughly half of those measured by Yamada (1975) on poled crystals. Thus the differences between the two sets of data in Table 1 may be attributed, at least in part, to the presence of 180° domains of millimeter size, or smaller. This is further corroborated by the fact that for the piezoelectric strain constant d_{22} calculated from the elastic constants and the piezoelectric stress constants of Table 1 pertaining to unpoled crystals a small value of 1.7×10^{-11} mV^{-1} is obtained, but that for poled crystals a value of 6.2×10^{-11} mV^{-1} has been measured by Yamada (1975) and a value of 8×10^{-11} mV^{-1} has been measured in this laboratory (see above, page 14).

From the data in Table 1 pertaining to unpoled crystals the ultrasonic transit time and its temperature coefficient were calculated as a function of the wave propagation direction in the a,b-, b,c- and a,c-planes, respectively. Temperature

TABLE 1

Elastic Constants $c^E_{\mu\nu}$ (10^{11} N/m^2), Piezoelectric Stress Constants $e_{i\mu}$ (C/m^2), Free Dielectric Constants ε^T_{ij} (dimensionless), Lattice Constants a, b, c (Å), and the Temperature Derivatives of these Quantities, $(\partial c^E_{\mu\nu}/\partial T)_p$ (10^8 dynes/cm°C) $(\partial e_i/\partial T)_p$ (10^{-3} C/m^2°C), $(\partial \varepsilon^T_{ij}/\partial T)_p$ ((°C^{-1}), $(1/a)(\partial a/\partial T)_p$, $(1/b)(\partial b/\partial T)_p$, $(1/c)(\partial c/\partial T)_p$ (10^{-5}(°C)$^{-1}$), for $Pb_2KNb_5O_{15}$ at 20°C.

Quantity M	M		$(\partial M/\partial T)$
	(Present*)	(Yamada**)	(Present)
c_{11}	1.027	1.61	-1.80
c_{22}	1.368	1.24	-2.16
c_{33}	1.456	1.66	+0.009
c_{44}	0.600	0.30	-0.50
c_{55}	0.398	0.63	-1.94
c_{66}	0.450	0.31	-0.76
c_{12}	0.232	0.41	+0.04
c_{13}	0.254	0.37	+0.38
c_{23}	0.196	0.45	-1.76
e_{16}	6.00	15	+13.27
e_{21}	0.84	1.4	-1.60
e_{22}	2.45	6.9	+0.27
e_{23}	0.94	0.4	-0.11
e_{34}	10.12	14	-3.33
ε^T_{11}	1465	1450	0.11
ε^T_{22}	1344	129	0.18
ε^T_{33}	1516	1550	0.40

Quantity L	L	(1/L)(∂L/∂T)
a	17.758	3.00
b	17.966	1.04
c	7.825	3.37

*Unpoled Crystals without 90° Domains, grown in this Laboratory by W. F. Regnault (1977)

**Poled Crystals (T. Yamada, J. Appl. Phys. 46, 2894-2898 (1975))

compensated directions for transverse modes are found for rotated Y cuts (rotated by angles of 18°, 25°, 68° and 77° around the X axis) with associated electromechanical coupling factors of 0.08, 0.07, 0.18 and 0.22, respectively. The maximum coupling factor of 0.24 occurs for the non-temperature compensated z-direction and is considerably smaller than the values of 0.73 reported by Yamada (1973; 1975). Again, the discrepancy seems to arise mostly from the presence or absence of submillimeter size 180° domains, but differences in crystal structure and/or composition could also be important. Hence it is likely that for poled crystals the coupling factors corresponding to the temperature compensated directions may also be considerably larger than for the unpoled crystals.

Although the largest coupling factor (0.22) found for a temperature dependent direction in $Pb_2KNb_5O_{15}$ is larger than the highest value calculated for α-$AlPO_4$ (0.17; Chang and Barsch, 1976) the superiority of PKN may be partly offset by its larger ultrasonic attenuation (Regnault, 1977).

3.2 α-Berlinite

Previously the elastic, thermoelastic and piezoelectric properties of α-berlinite have been measured and used to calculate temperature compensated cuts for bulk acoustic waves with orientations similar to those of α-quartz, but with electromechanical coupling factors up to 2.5 times larger than for quartz (Chang and Barsch, 1976). However, the piezoelectric constants determined from ultrasonic velocity measurements are subject to relatively large error, since the piezoelectric stiffening term in the Kristoffel tensor is obtained as the difference between large quantities. Furthermore, the analysis of the ultrasonic data and the calculation of the temperature compensated directions and of the electromechanical coupling factor are based on the simplifying assumption that the two dielectric constants ε_{11}^T and ε_{33}^T are equal. For these reasons independent measurements of the piezoelectric and dielectric constants of berlinite were made under the present contract.

3.2.1 Piezoelectric Constants

The piezoelectric strain constants d_{11} and d_{14} were determined by the x-ray method first used by Bhalla et al. (1971) for measuring d_{11} for α-quartz in good agreement with data obtained by other authors. For this purpose a pentagon-shaped x-cut platelet with face orientation, dimensions and shape as shown in Figure 7 was prepared from the same crystal that was used for the earlier ultrasonic measurements (Chang and Barsch, 1976). The two

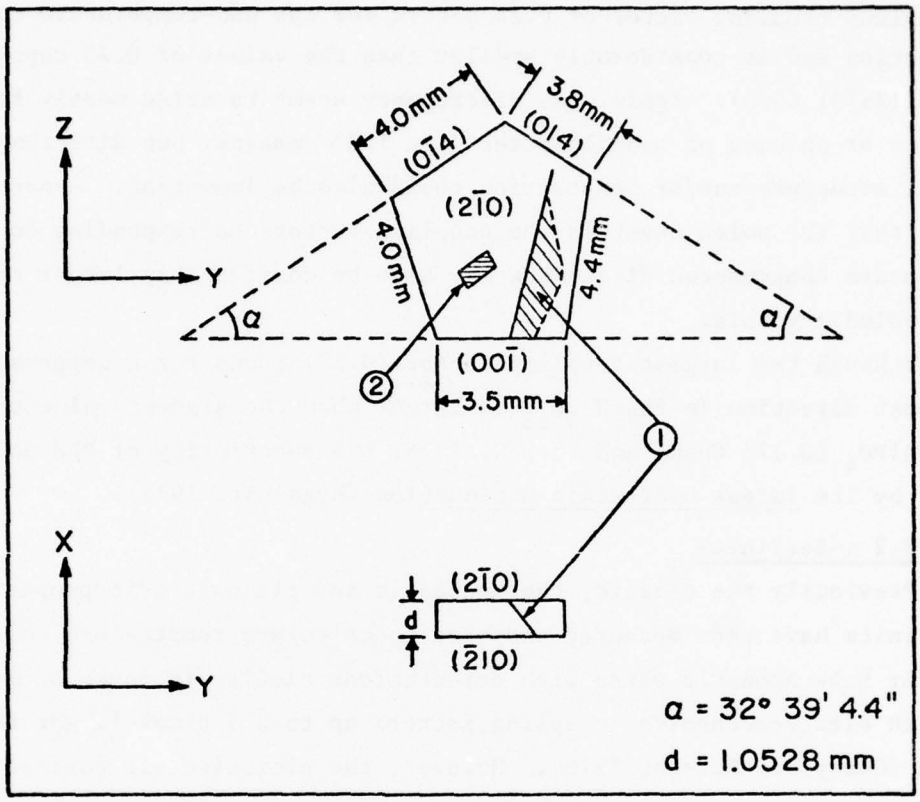

Fig. 7 Dimensions, orientation and shape of X-cut platelet of berlinite sample XP-2 used for x-ray determination of piezoelectric constants. The orientation of the right-handed cartesian coordinate system corresponds to the 1949 IRE convention (IRE 1949). The large pentagon shaped faces (2$\bar{1}$0) and ($\bar{2}$10) were electroded with vapor deposited aluminum. (1) indicates a crack and (2) an area with different light reflection on the aluminum electrode.

pentagon-shaped faces $(2\bar{1}0)$ and $(\bar{2}10)$ (or, equivalently, $(\bar{1}\bar{1}0)$ and (110)) were plated with evaporated aluminum electrodes. The platelet as prepared originally was larger than shown in Fig. 7 but it contained Dauphin twins, that were identified by means of the different etch patterns observed on the $(2\bar{1}0)$ and $(\bar{2}10)$ faces. After removal of the twinned regions the shape shown in Fig. 7 resulted. The remaining platelet contained a crack which was not removed since it was feared that this would result in a specimen too small for the measurement of the transverse piezoelectric effect.

The measurements were made by measuring the changes of the Bragg angles of the $4\bar{2}0$, of the $0\bar{1}4$, and of the 014 reflections caused by application of a static voltage of ± 2000V to the electroded faces. Details of the data analysis have been given before (Barsch and Spear, 1977). The following steps were taken in order to reduce systematic errors:

(1) The x-ray tube has been adjusted for maximum intensity by positioning it at the Bragg angle of the monochrometer crystal.

(2) The zero position (corresponding to $\theta = 0$) of the sample was checked by adjusting the position of the monochromator and the angular position of the sample such that the x-ray beam grazes the sample surface (Fig. 8a).

(3) The proper positioning of the sample surface so as to coincide with the rotation axis was checked by verifying the zero position according to (2) after rotation of the sample by 180°, together with a reflected laser beam (Fib. 8b).

(4) The position of the spring attached to the turning arm of the turntable was changed and the spring tension was reduced in order to reduce both the restoring torque and the force normal to the axis of the turntable.

Other precautions found necessary and taken earlier include

(1) elimination of the driving motor and manual rotation of the goniometer turntable in steps of 5 seconds of arc,

(2) very gradual opening of the valve for the cooling water for the x-ray tube in order to avoid any mechanical shock causing small changes in the position of the x-ray tube,

(3) a waiting period of about 1 to 2 hours after turning on the power supply of the x-ray tube until thermal equilibrium is reached,

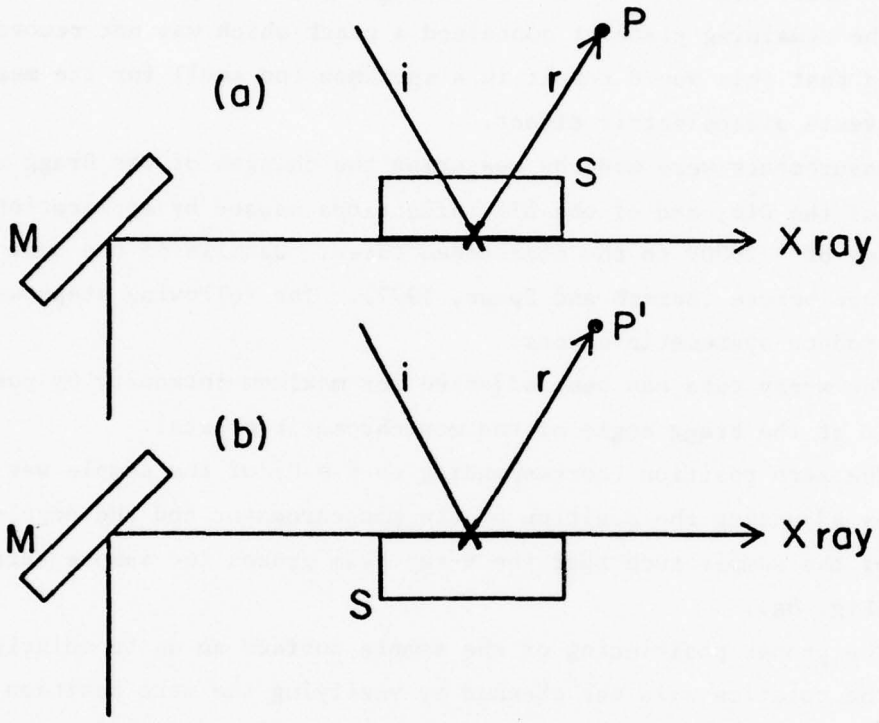

Fig. 8. Method for aligning crystal specimen.
(a) Position of glass sample used for checking zero position corresponding to zero Bragg angle.
(b) Rotated glass sample position for checking coincidence of sample surface with rotation axis of gomiometer.
Incident (i) and reflected (r) laser beam as shown indicate absence of tilt angle of sample if points P and P' coincide. For laser beam check the glass sample surface coinciding with the rotation axis x is aluminum plated.

(4) most measurements were made during evening and night hours and on weekends in order to reduce the effect of voltage fluctuations present in the electrical network.

Increasing the accuracy by increasing the voltage above 2000 V proved unsuccessful because of dielectric breakdown which caused cracking of the sample.

The expressions for the change of the Bragg angle θ with electric field E resulting from the longitudinal or transverse piezoelectric effect are given by (Barsch, 1976)

$$-\cot\theta\left(\frac{\partial\theta}{\partial E}\right) = \begin{cases} L\ (\vec{\alpha} \parallel \vec{N}) \\ T\ (\vec{\alpha} \perp \vec{N}) \end{cases} \tag{3}$$

Here $\vec{\alpha}$ is the unit vector in the direction of the electric field, $\vec{N}$ the normal of the reflecting lattice plane, and

$$L = N_r N_i N_j \ d_{rij} \tag{4a}$$

$$T = \alpha_r N_i N_j \ d_{rij} \tag{4b}$$

are the coefficients for the longitudinal and transverse piezoelectric effect, respectively. The coefficients d_{rij} are the piezoelectric strain constants in tensor notation, and the summation convention is implied in equs. (4a) and (4b).

For the X-cut platelet sample X-2 and for the coordinate system of Fig. 7 it is $\vec{\alpha} = (1,0,0)$. For the crystal class D_3 the lattice planes parallel to the X-face of this sample correspond to Miller indices of the form hkl = $(2h\ \bar{h}\ 0)$, so that equ. (4a) becomes (Barsch, 1976):

$$L = d_{11} \tag{5a}$$

For Miller indices of the form hkl = 0kl equ. (4b) becomes for the class D_3

$$T = -\eta^2 d_{11} + \eta J\, d_{14} \tag{5b}$$

where $N = (0, \eta, J)$ with

$$\eta = \frac{2k}{aR} \tag{6a}$$

$$J = \frac{1}{cR} \tag{6b}$$

and

$$R = \left[\frac{4}{3}\left(\frac{k}{a}\right)^2 + \left(\frac{l}{c}\right)^2\right]^{1/2} \qquad (6c)$$

a,c denote the lattice parameters. The two faces $(0\bar{1}4)$ and (014) of the sample X-2 were chosen so as to maximize the coefficient ηJ of d_{14} in equ. (5b). With the lattice parameters of berlinite (a = 4.943 Å, c = 10.974 Å; Chang and Barsch, 1976) the lattice plane normal is for $(hk\ell) = (0,\pm 1,4)$ given by $\vec{N} = (0, \pm \sin\alpha, \cos\alpha)$ with $\alpha = 32°39'4.4''$ and the coefficients in equ. (5b) become

$$\eta^2 = 0.29109 \qquad (7a)$$

$$\eta J = \pm\ 0.45426 \qquad (7b)$$

where the upper sign refers to the (014) face, and the lower one to $(0\bar{1}4)$.

In Table 2 the values for the Bragg angle θ, for the change of the Bragg angle $\Delta\theta$ caused by a total potential difference of 4000V, and for the measured values of the longitudinal and transverse piezoelectric effect according to equs. (4a) and 4b) are listed for the reflections $4\bar{2}0$, $0\bar{1}4$ and 014. The values of L and T are averages over four to ten successful runs. Each run is the result of about 20 consecutive measurements of the line profiles of the Bragg peak obtained with alternating electric field values corresponding to applied voltages of ±2000V. A run was considered successful if the plot of the line center positions for the Bragg peaks of successive measurements versus the number of the run resulted in two parallel straight lines as shown in Fig. 5 of our Final Technical Report on Contract No. F19628-75-C-0085 (Barsch and Spear, 1977). For reasons discussed below only a fraction of all attempted runs was successful. Usually the Bragg reflections of the x-ray beam for the various runs occurred from different areas of the crystal surface.

From the data in Table 2 one obtains in connection with equs. (3), (5a) and (5b), and (7a) and (7b) the following 3 equations for the piezoelectric constants d_{11} and d_{14} (in units of 10^{-11} m/V):

$$d_{11} = -1.167 \qquad (8a)$$

$$-0.29109\ d_{11} - 0.45426\ d_{14} = 0.817 \qquad (8b)$$

$$-0.29109\ d_{11} + 0.45426\ d_{14} = -0.127 \qquad (8c)$$

From equs. (8b) and (8c) one obtains by eliminating d_{14} for d_{11} a value of 1.183, in good agreement with the independent value according to equ. (8a), indicating good internal consistency of the three independent sets of measurements.

TABLE 2

Bragg angles θ (in degrees), change of Bragg angle $\Delta\theta$ (in seconds) for total potential difference of 4000V, and magnitude of the longitudinal (L) or transverse (T) piezoelectric effect given by $-\cot\theta\,(\partial\theta/\partial E)$ for 3 reflections

Reflection	θ	$\Delta\theta$	Type	$-\cot\theta\left(\frac{\partial\theta}{\partial E}\right)$
$4\bar{2}0$	38.559	6.54	L	-1.167
$0\bar{1}4$	19.518	-2.27	T	+0.817
014	19.518	+0.352	T	-0.127

The best solution of equs. (1a) to (1c) is taken as

$$d_{11} = (-1.17 \pm 0.04) \times 10^{-11}\ \frac{m}{V} \tag{9a}$$

$$d_{14} = (-1.04 \pm 0.06) \times 10^{-11}\ \frac{m}{V} \tag{9b}$$

Calculating the piezoelectric stress constants e_{11} and e_{14} from the relations

$$e_{11} = (c_{11} - c_{12})\, d_{11} + c_{14}\, d_{14} \tag{10a}$$

$$e_{14} = 2c_{14}\, d_{11} + c_{44}\, d_{14} \tag{10b}$$

and using the ultrasonic elastic constant values (Barsch and Chang, 1976)

$$c_{11} - c_{12} = 0.568 \times 10^{11}\ N/m^2 \tag{11a}$$

$$c_{44} = 0.432 \times 10^{11}\ N/m^2 \tag{11b}$$

$$c_{14} = -0.124 \times 10^{11}\ N/m^2 \tag{11c}$$

gives

$$e_{11} = (-0.54 \pm 0.02)\ C/m^2 \tag{12a}$$

$$e_{14} = (-0.16 \pm 0.03)\ C/m^2 \tag{12b}$$

For comparison the ultrasonically determined values (Chang and Barsch, 1976) are also given here:

$$e_{11} = (\pm 0.30 \pm 0.06)\ \frac{C}{m^2} \qquad (13a)$$

$$e_{14} = (\mp 0.13 \pm 0.13)\ \frac{C}{m^2} \qquad (13b)$$

Here the upper and lower signs belong together, respectively.

For righthanded quartz the signs of the piezoelectric and elastic constants are for the choice of axes according to the IRE standards (IRE, 1949) as follows.

$$d_{11} < 0 \qquad e_{11} < 0$$

$$d_{14} < 0 \qquad e_{14} > 0$$

$$c_{14} < 0$$

For lefthanded quartz all signs, except for c_{14} are opposite to those for right-handed quartz. Furthermore, for righthanded quartz "on extension the positive ends of the a-axes, and therefore of the x-axes, become negatively charged" (IRE, 1949). According to equs. (9) and (12) for our berlinite sample the four piezoelectric constants d_{11}, d_{14}, e_{11}, e_{14} are all negative, and the ultrasonically measured elastic constant c_{14} is also negative, provided the orientation of axes for berlinite can be based on the same criteria for the formation of the rhombo-heral faces as for quartz (the axes x,y,z form a right-handed cartesian system, with the x-axis parallel to one of the a-axes, such that the y-axis is below a minor rhombohedral face), and further provided that the diffraction pattern caused by etch pits as observed through an oriascope is the same for right-quartz and for right-berlinite. Although it was not possible to determine the handedness of our berlinite sample directly by placing a c-cut sample between crossed polaroids the above mentioned evidence seems to suggest beyond any reasonable doubt (a) that our present berlinite is right-handed (as previously concluded, Chang and Barsch, 1976) and (b) that in all respects, except for the sign of e_{14} the criteria for determining the handedness and choosing the axes are the same for berlinite and quartz. Furthermore it may be concluded that the orientation of axes for the berlinite sample used for the x-ray determination of the piezoelectric constants corresponds to that of Fig. 7.

Comparison of the x-ray values (12) with the ultrasonic values (13) for the piezoelectric constant shows the following

(a) The static x-ray value for e_{11} is 80% larger than the ultrasonically determined dynamic value, but the joint experimental error of both values amounts

only to 27% of the smaller of the two values. This indicates that either one or both of the errors given in (12) and (13) are underestimated.

(b) The magnitude of the x-ray value for e_{14} is 22% larger than the ultrasonic value, but has the opposite sign. Again the discrepancy is larger than the joint experimental error, however, because of the large error of 100% of the ultrasonic value this value could be discarded altogether.

The most serious unaccounted systematic error of the x-ray results is believed to arise from sample inhomogeneities associated with variations in stoichiometry, impurities, and microscopically small inclusions and microcracks. These crystal imperfections could give rise to significant deviations from the spatially homogeneous strain and electric field which form the basis for the above theoretical equations used in the analysis of the data. It is believed that the unsuccessful and non-reproducible runs that were discarded in the data analysis are associated with crystal imperfections and, especially, space charge effects. This conjecture is corroborated by the occurrence of space charge effects in the measurement of the piezoelectric constants of α-quartz by using a capacitance dilatometer (Hauris, 1978). On the other hand, since it was possible to obtain reproducible and mutually consistent values for various independent runs for each of the three crystal faces measured it is probable that the measured x-ray values of the piezoelectric constants are actually representative of the particular berlinite sample measured. However, systematic errors that cannot be discarded could be space charge effects, field enhancement by crystal imperfections and a possible frequency dependence of the piezoelectric constants through defect relaxation mechanisms.

3.2.2 Electromechanical Coupling Factor

Since it has been possible to obtain an internally consistent set of piezoelectric constants by means of the x-ray method for α-berlinite, and since the suitability of the x-ray method has also been verified for the piezoelectric constants of α-quartz (see below section 3.3) the values for d_{11} and d_{14} given in equs. (9a) and (9b) may be accepted with some degree of confidence. Therefore the electromechanical coupling factor of berlinite for the rotated Y-cut has been calculated as a function of orientation by using the x-ray data of the piezoelectric constants in conjunction with the previous ultrasonic elastic and thermoelastic data (Chang and Barsch, 1976). The associated temperature coefficient of the resonance frequency was also calculated for four plausible choices of the temperature coefficients of the piezoelectric stress constants. The results show that the temperature compensated directions do not change drastically with these input data.

In Fig. 9 the calculated coupling factor for the rotated Y-cut is shown as a function of the rotation angle. Also indicated are the values corresponding to the BT cut and AT cut, calculated from the assumption $(\partial e_{11}/\partial T) = (\partial e_{14}/\partial T) = 0$. This curve should supersede Fig. 6 of our previous paper on berlinite (Chang and Barsch, 1976). Comparison of these two figures allows the following conclusions to be drawn.

(1) The maximum value of k does not occur near $\phi = 0$, corresponding to the Y-cut, but at $\phi = 17°$.

(2) The minimum value of k does not occur at $\phi = +65°$, but at $\phi = -73°$.

(3) The maximum value $k_{max} = 0.433$ for $\phi = 17°$ is almost twice as large as the previously reported value of 0.233 and 3.2 times larger than the maximum value of quartz (0.135).

(4) The value of $k_{BT} = 0.13$ for the BT cut is roughly the same as previously reported (0.134), but the value of $k_{AT} = 0.40$ for the AT cut is 2.65 times larger than the previously reported value (0.151) and 4.5 times larger than the value for AT cut quartz (0.089).

The greatly increased value of k_{AT} results both from the larger x-ray value of e_{11} and from the negative sign of the x-ray value of e_{14} which results in the shift of the minimum value of k from positive values of ϕ (as for α-quartz and as previously reported for α-berlinite) to a negative value of ϕ.

The results displayed in Fig. 9 should be considered as preliminary until revised elastic and thermoelastic data are determined for this purpose from the least squares analysis of our previous ultrasonic data with the piezoelectric constants from the x-ray measurements used as input.

3.2.3 Dielectric Constant

The dielectric constant ε_{33}^{T} and the loss tangent $\tan\delta$ have been measured from -175° to +200°C at frequencies of 10^3, 10^4, 10^5 and 10^6 Hz. For this purpose a c-cut platelet of area 3.34 mm^2 and thickness 0.0968 mm of α-berlinite was used which had been grown hydrothermally at the Naval Weapons Center, China Lake, California. Gold was used as electrode material and was deposited by evaporation. No chemical analysis was made for comparison with the sample used for the ultrasonic and x-ray measurements. The dielectric measurements were performed with an automatic Hewlett Packard capacitance bridge Model 4270A. All data were taken with increasing and decreasing temperature, and no thermal hysteresis was observed.

In Figs. 10a to 10d the results for the four frequencies measured are plotted as a function of temperature. It is apparent that one relaxation peak occurs in the loss tangent which is associated with the usual step-like kink in

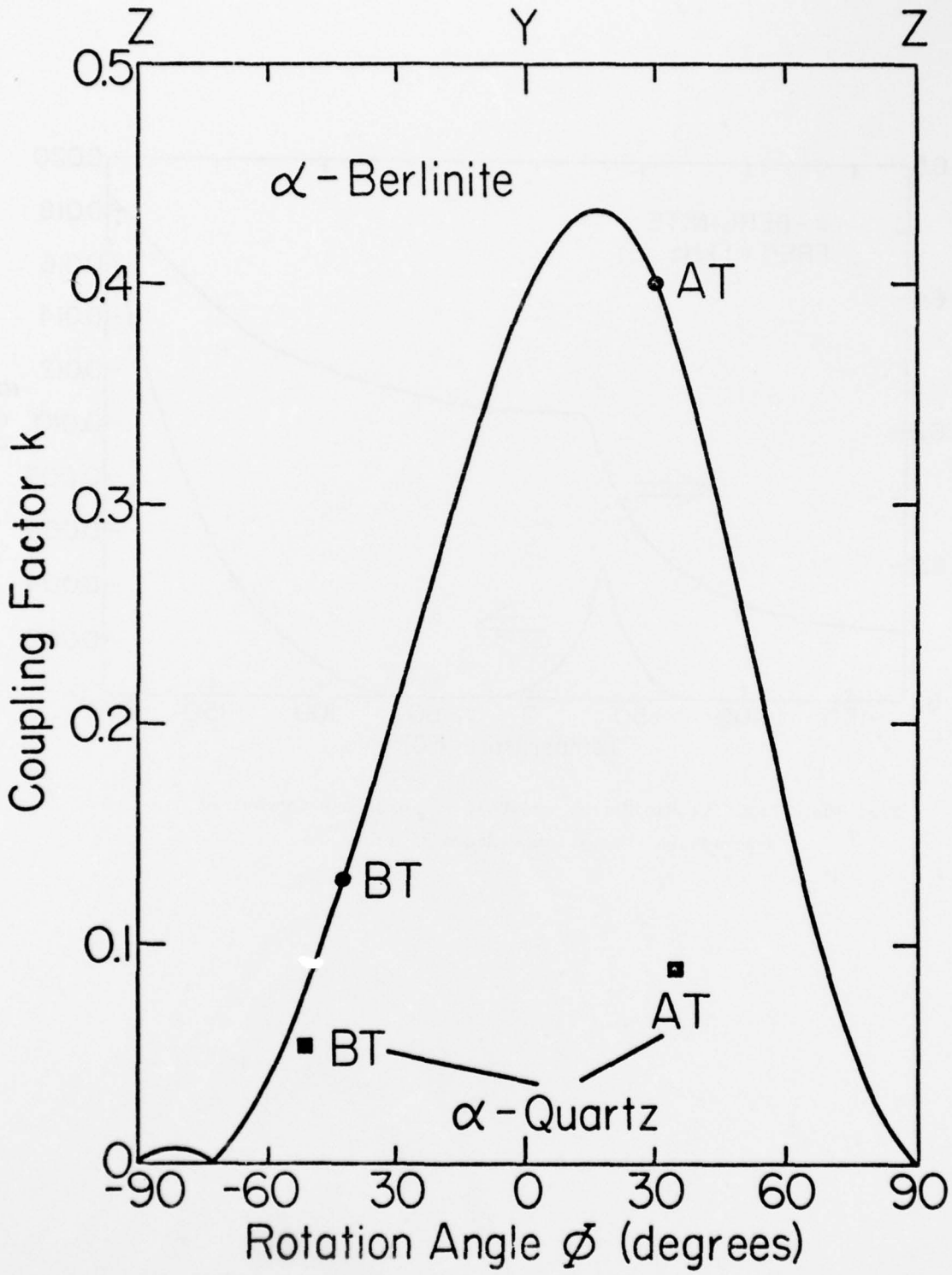

Fig. 9. Electromechanical coupling factor k for rotated y-cut of α-berlinite versus angle of rotation Φ, calculated from x-ray data of piezoelectric constants.

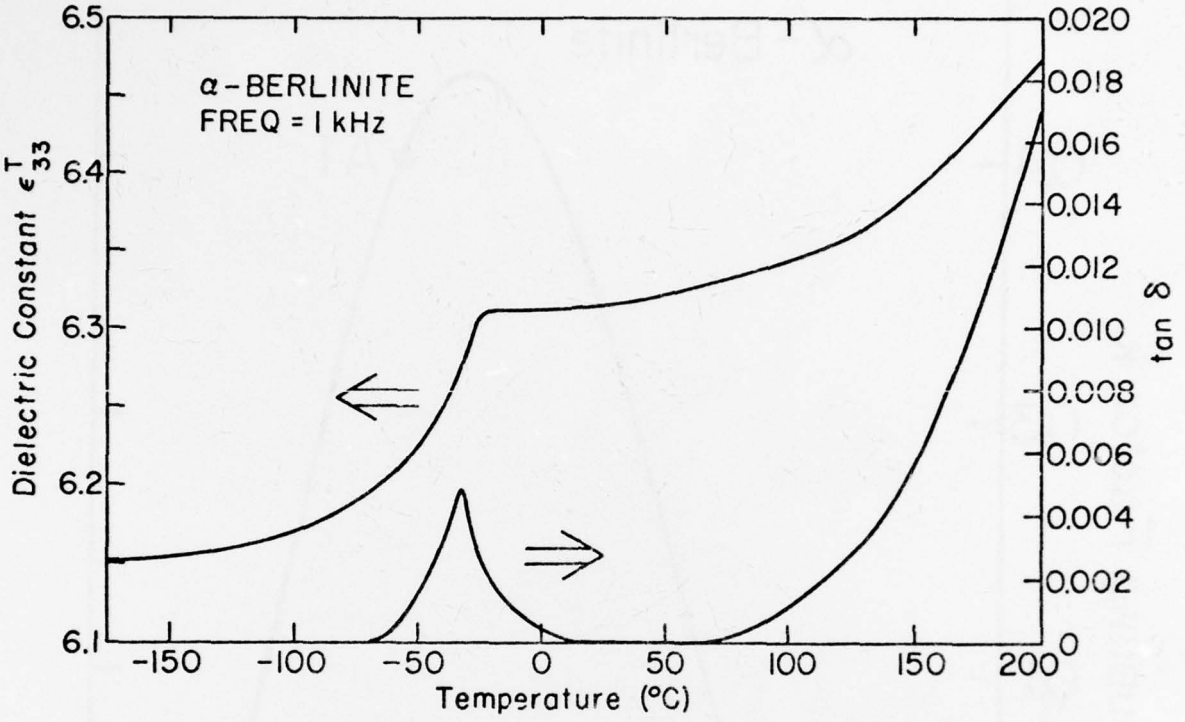

Fig. 10a. Relative dielectric constant ϵ_{33}^T and loss tangent of α-berlinite versus temperature at 1 kHz.

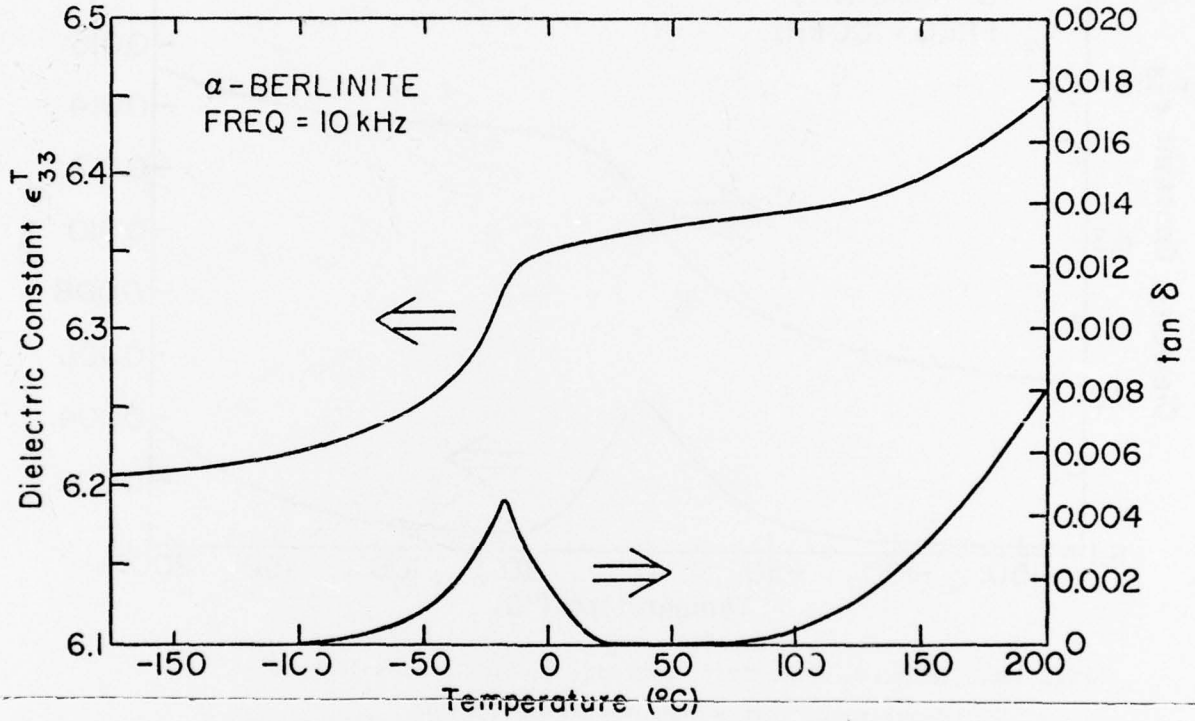

Fig. 10b. Relative dielectric constant ε_{33}^T and loss tangent of α-berlinite versus temperature at 10 kHz.

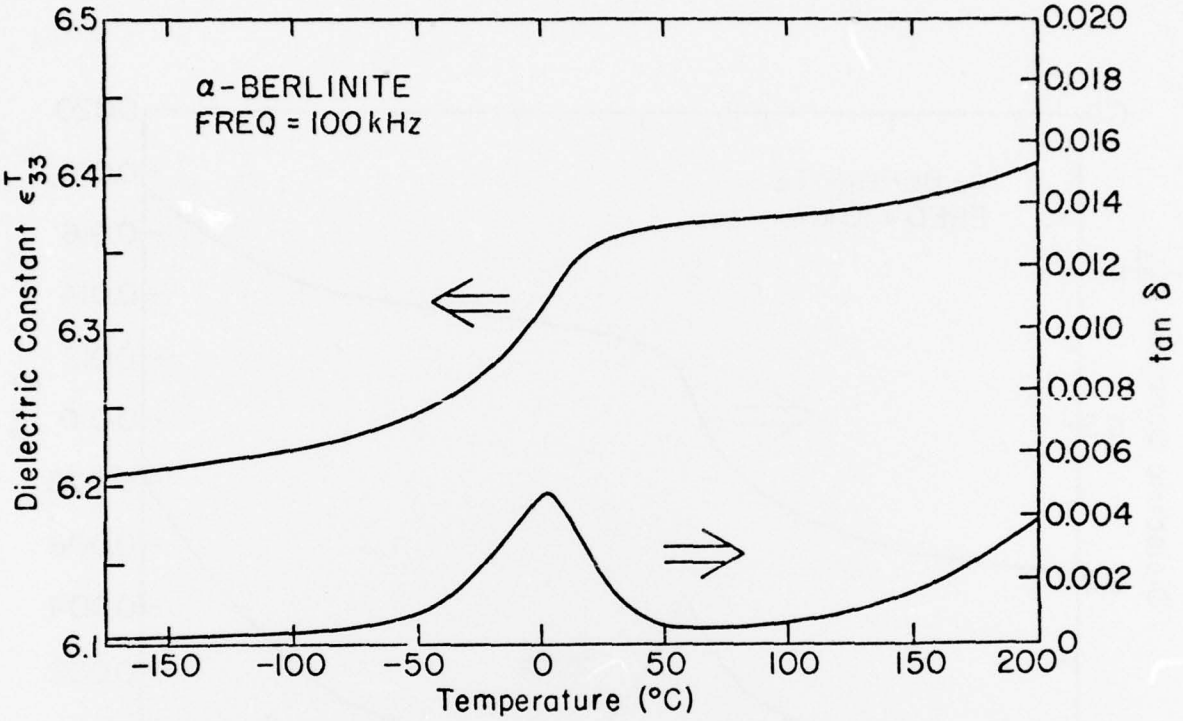

Fig. 10c. Relative dielectric constant ε_{33}^T and loss tangent of α-berlinite versus temperature at 100 kHz.

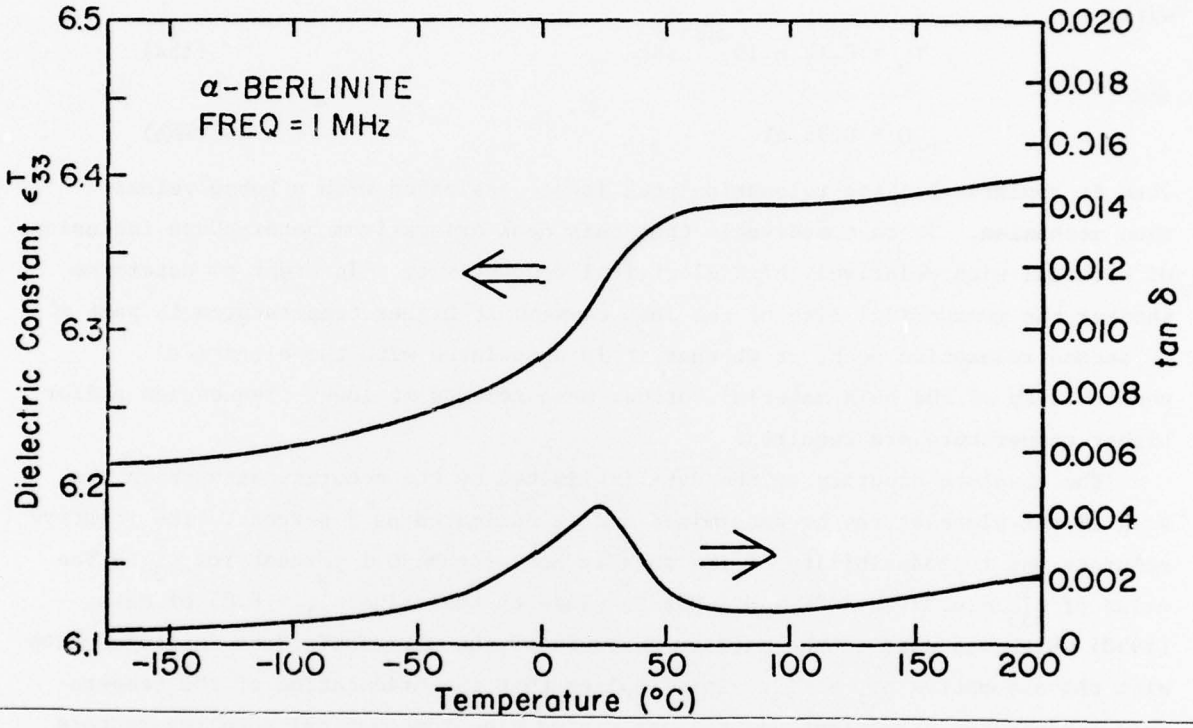

Fig. 10d. Relative dielectric constant ε^T_{33} and loss tangent of α-berlinite versus temperature at 1 MHz.

the real part of the dielectric constant, and a continuous rise of tan δ at higher temperature, which is associated with a continuous rise of the real part. The Cole-Cole plot of the data near the relaxation peak at lower temperature gives a circle with its center shifted below the abscissa. The relaxation time can be described by an exponential temperature dependence of the form

$$\tau = \tau_o \, e^{Q/kT} \tag{14}$$

with

$$\tau_o = 0.31 \times 10^{-19} \text{ sec} \tag{15a}$$

and

$$Q = 0.75 \text{ eV} \tag{15b}$$

Thus it appears that the relaxation peak is not assicated with a Debye relaxation mechanism. It is conceivable that this peak arises from heterophase inclusions of material with relatively high electrical conductivity. In order to determine whether the monotomical rise of the loss tangent at higher temperatures is part of a second relaxation peak, or whether it is associated with the electrical conductivity of the bulk material further measurements at lower frequencies and/or higher temperature are required.

The absolute accuracy of the data is limited by the accuracy with which the area of the platelet can be determined and is estimated as 5 percent. The relative accuracy and reproducibility of the data is better than 0.1 percent for ε_{33}^T. The value of $\varepsilon_{33}^T = 6.32$ at 20°C and 1 MHz is close to the value $\varepsilon_{11}^T = 6.05$ of Mason (1950) which was used in the earlier analysis of the ultrasonic data in conjunction with the assumption $\varepsilon_{11}^T = \varepsilon_{33}^T$. This implies that the orientation of the temperature compensated directions and the associated electromechanical coupling factors determined earlier are not changed significantly. However, the presence of the relaxation effect increases the temperature coefficient $(\partial \varepsilon_{33}^T / \partial t)$ by about two orders of magnitude near the inflection point of ε_{33}^T, as compared with the value obtained after subtracting the contribution from the relaxation contribution. Since for 1 MHz this inflection point is at 20°C, and since for higher frequencies it is not too far above room temperature it is to be expected that the exact orientation of the temperature compensated directions and the associated values of the electromechanical coupling factor depend both on the frequency and on the nature and concentration of the crystal defects. Further work is required in order to assess the magnitude of these effects.

3.3 X-Ray Method for Determination of Piezoelectric Constants

In order to check the reliability of the x-ray method for measuring the piezoelectric strain constants this method has been applied to α-quartz, for which experimental data obtained by other methods are available. For this purpose two X-cut platelets of quartz with a shape similar to the X-cut platelet of α-berlinite depicted in Fig. 7 and of linear dimensions of about 3 mm were prepared. However, for the measurement of the transverse piezoelectric effect the $(0\bar{1}2)$ and (012) faces were used in quartz because they correspond roughly to the same Bragg angles as the $(0\bar{1}4)$ and (014) faces in berlinite, respectively. The thickness of the two platelets was about 0.83 mm.

Whereas for berlinite it has been possible to obtain three independent fairly reproducible series of runs for the $(2\bar{1}0)$, $(0\bar{1}4)$ and (014) faces for quartz it was only possible to obtain fairly reproducible series of runs for the $(2\bar{1}0)$ and $(01\bar{2})$ faces, but not for the $(0\bar{1}2)$ face. Moreover, the results for quartz tended to be less reproducible than for berlinite, especially for the transverse effect. It was noted that the reproducibility was considerably increased if the specimen was kept in vacuum at room temperature for about 24 hours prior to the measurements, and if the measurements were conducted in an atmosphere of circulating nitrogen gas. This seems to suggest changes in the microscopic electric field caused by adsorption and/or diffusion of water vapor or hydroxyl ions at surface cracks and bulk flaws that extend to the surface. Similar observations have been made, and similar conclusions have been drawn by Hauris (1979) in the course of measurements of the longitudinal coefficient d_{11} of α-quartz by means of a capacitance dilatometer.

The x-ray measurement of the piezoelectric constant d_{14} in the present work was possible only after it was realized that of the two configurations for measuring the transverse piezoelectric effect shown in Fig. 11 configuration (a) corresponds to a smaller half-width of the K_{α_1} peak (about 1 minute of arc) than configuration (b) (about 2 minutes of arc). Therefore for measuring the small shift of about 0.3 seconds of arc induced by an electric field difference of 4000V per 0.88 mm configuration (a) provides greater accuracy than configuration (b). This assymmetry is apparently caused by the spectral asymmetry of the primary x-ray beam.

From a total of about 40 runs with the two platelets, which involved different geometrical configurations for the monochromator crystal and for the quartz crystal platelets a value of

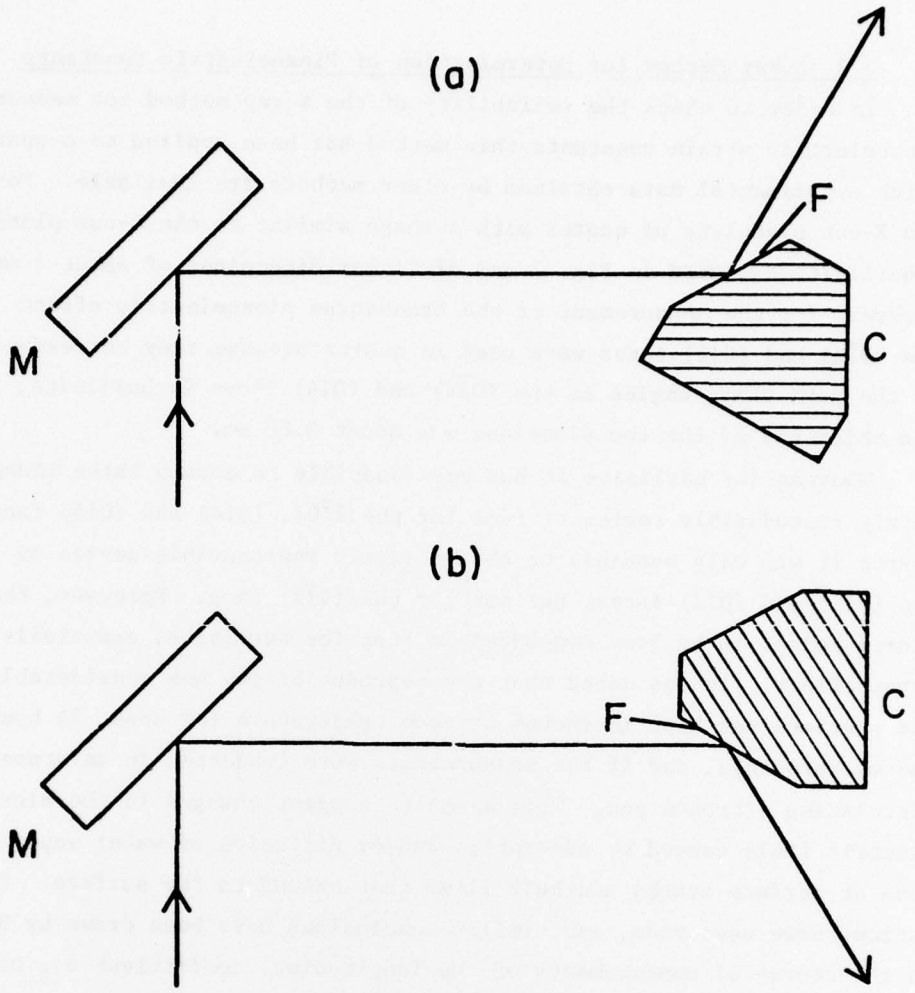

Fig. 11. Two alternate configurations for measuring the transverse piezoelectric effect (Schematic). M - Monochromator; C - Electrode Plated Sample Crystal; F - Crystal Face. The arrows indicate the x-ray beam.
Configuration (a) corresponds to a smaller half-width of the K_{α_1} peak (about 1 minute of arc) than configuration (b) (about 2 minutes of arc).

$$d_{11} = (-2.29 \pm 0.04) \times 10^{-12} \text{ m/V} \qquad (16a)$$

was determined from the $(2\bar{1}0)$ reflection for α-quartz. This value is in good agreement with the values obtained by the resonance method, namely (in units of 10^{-12} m/V) 2.29 (Cook and Weissler, 1950), 2.25 (Mason, 1950) and 2.31 (Bechman, 1958).

From four successful runs for the transverse effect as measured with the (024) reflection in conjunction with (16a) a value of

$$d_{14} = (-1.10 \pm 0.1) \times 10^{-12} \text{ m/V} \qquad (16b)$$

has been determined. This value is somewhat larger than the values obtained by the resonance method, which range from 0.68×10^{-12} m/V (Cook and Weissler, 1950) to 0.85×10^{-12} m/V (Mason, 1950). The difference between the two sets of values could possibly be attributed to sample inhomogeneities and associated fluctuations in the microscopic electric field. It should also be noted that for the values of d_{14} obtained by the resonance method a larger spread is observed than for d_{11}. This could indicate that through the effect of crystal imperfections d_{14} is more sample dependent than d_{11}, but it could also indicate that the measurement of d_{14} by means of the transverse piezoelectric effect is intrinsically less accurate than the measurement of d_{11} by means of the longitudinal effect, no matter whether the x-ray method or the resonance method is used.

As mentioned above, it has not yet been possible to obtain consistent values for d_{14} by Bragg reflection from the $(0\bar{1}2)$ face of the quartz specimen, even if the specimens were kept in vacuum prior to the measurement. The reasons for the different behavior of the (012) and $(0\bar{1}2)$ faces are not yet understood. Since these two faces possess different surface energies, and chemical activities, as is evident from their different growth habits, the difficulties with the piezoelectric measurements could perhaps be attributed to the presence of crystal imperfections, especially water molecules or hydroxyl ions which are affected differently by the two types of surfaces.

Possible future improvements in measuring the piezoelectric constants include the following steps.

(1) Degassing of the crystal specimen in vacuum and at elevated temperature before they are electrode-plated.

(2) Performing the electrode-plating and the actual x-ray measurements in vacuum.

(3) Reducing the line width of the Bragg peak by using a double or triple monochromator, that is by double or triple reflection of the primary x-ray beam from the monochromator crystal.

In summary, it can be said that the suitability of the x-ray method has been established for the longitudinal piezoelectric effect. For the transverse effect, however, both the resonance method and the x-ray method show larger variations, that could arise either from the relative smallness of the effect and/or from the relatively stronger dependence of the transverse effect on structural imperfections or contamination of the specimen.

4. Conclusions

The results obtained under the present contract indicate that temperature compensated performance and large electromechanical coupling factors in ultrasonic bulk and surface wave devices are not mutually exclusive, and that the performance characteristics of presently used acoustic wave devices are not yet optimized with respect to the choice of the best possible material. The results indicate further that the approach used in our systematic search for new temperature compensated piezoelectric materials with larger piezoelectric coupling than α-quartz has been very successful. This approach led to the identification of α-berlinite and lead potassium niobate as superior substitutes for α-quartz and consisted of the following four steps:

(1) Selection of promising candidate materials on the basis of heuristic criteria,

(2) Growth of single crystal specimen sufficiently large for physical property measurements,

(3) Measurement of the complete set of the elastic, piezoelectric, dielectric and thermoelastic constants,

(4) Computer calculations to determine the temperature compensated directions and their associated coupling factors for bulk and surface acoustic waves.

It is to be expected that through a continued systematic search new materials with still better properties could be found.

5. Recommendations

Since α-berlinite and lead potassium niobate have been found to be superior to α-quartz for bulk and surface wave applications it would be appropriate to continue work on both materials in order to optimize their properties. This would

involve better control of the crystal growth parameters required for production of high-quality crystals and further investigations on the effect of crystal imperfections and chemical composition on the properties and performance.

In addition, it appears promising to continue the systematic search for new temperature compensated materials on the basis of the approach used previously, which could lead to the discovery of other materials with still better properties. Specifically, it is recommended to continue crystal growth efforts for subsequent property measurements on Li_2SiO_3 and $Bi_2PbNb_2O_9$ in addition to lead potassium niobate.

6. References

BARSCH, G.R. (1976). X-ray Determination of Piezoelectric Constants, Acta Cryst. A32, 575-586.

BARSCH, G.R. and NEWNHAM, R.E. (1975). Piezoelectric Materials with Positive Elastic Constant Temperature Coefficients, AFCRL-TR-75-0163; Final Report on Contract No. F19628-73-C-0108.

BARSCH, G.R. and SPEAR, K.E. (1977). Temperature Compensated Piezoelectric Materials. RADC-TR-77-179; Final Technical Report on Contract No. F19628-75-C-0085, A044237.

BECHMANN, R.A. (1958). Elastic and Piezoelectric Constants of α-Quartz. Phys. Rev. 110, 1060-1061.

BHALLA, A.S., BOSE, D.N., WHITE, E.W. and CROSS, L.E. (1971). Precise X-ray Determination of Small Homogeneous Strains Applied to the Direct Measurement of Piezoelectric Constants. phys. stat. sol. (a)7, 335-339.

CHANG, Z.P. and BARSCH, G.R. (1976). Elastic Constants and Thermal Expansion of Berlinite, IEEE Proc. Sonics Ultrasonics, SU23, 127-135.

COOK, R.K. and WEISSLER, P.G. (1950). Piezoelectric Constants of α- and β-Quartz at Various Temperatures. Phys. Rev. 80, 712-716.

HAURIS, J. (1978). MS Thesis in Solid State Science, The Pennsylvania State University.

IRE (1949). Standards on Piezoelectric Crystals. Proc. IRE 14, S1, 1378.

MASON, W.P. (1950). Piezoelectric Crystals and Their Applications to Ultrasonics (Van Nostrand, New York).

NAKANO, J. and YAMADA, T. (1975). Ferroelectric and Optical Properties of Lead Potassium Niobate. J. Appl. Phys. 46, 2361-2365.

REGNAULT, W.E. (1977). Elastic, Piezoelectric, Dielectric and Optical Properties of Lead Potassium Niobate. Ph.D. Thesis in Physics, The Pennsylvania State University.

YAMADA, T. (1973). Single-Crystal Growth and Piezoelectric Properties of Lead Potassium Niobate. Appl. Phys. Lett. 23, 213-214.

YAMADA, T. (1975). Elastic and Piezoelectric Properties of Lead Potassium Niobate. J. Appl. Phys. 46, 2894-2898.

MISSION
of
Rome Air Development Center

RADC plans and executes research, development, test and selected acquisition programs in support of Command, Control Communications and Intelligence (C^3I) activities. Technical and engineering support within areas of technical competence is provided to ESD Program Offices (POs) and other ESD elements. The principal technical mission areas are communications, electromagnetic guidance and control, surveillance of ground and aerospace objects, intelligence data collection and handling, information system technology, ionospheric propagation, solid state sciences, microwave physics and electronic reliability, maintainability and compatibility.

Printed by
United States Air Force
Hanscom AFB, Mass. 01731